Miniature ionization chamber detector developed for X-ray microprobe measurements

M. Kocsis[a]* and A. Somogyi[b]

[a]Instrument Support Group, European Synchrotron Radiation Facility, 38043 Grenoble CEDEX, France, and [b]Department of Chemistry, University of Antwerp, B-2610 Antwerp, Belgium. E-mail: kocsis@esrf.fr

A windowless small ionization chamber detector has been developed for monitoring the intensity of the microbeam at the ID18F microprobe end-station of the European Synchrotron Radiation Facility. The small dimensions of the ionization chamber (10 mm along the beam direction and 5 mm perpendicular to it) make it possible to place it very close to the sample. A pinhole of diameter 50 µm was used for defining the entrance window of the ionization chamber; thus the small counter can be used as an order-selecting aperture while measuring simultaneously the intensity after the aperture. In the present work the technical characteristics, such as the current–voltage curve, stability and linearity, of the small monitor have been tested.

Keywords: windowless ionization chambers; microprobe; intensity monitors; microbeams.

1. Introduction

The reliable monitoring of the intensity of the X-ray beam in the case of synchrotron-radiation-induced measurements is essential in following and correcting for the decrease of the synchrotron current and the intensity change caused by the different optical and beam-shaping elements. In order to probe precisely the change in the intensity of the X-ray radiation penetrating the sample, a counter should be introduced between the last optical or beam-shaping element and the sample. This requirement can be very difficult to fulfill, especially with commercially available detectors and in the case of microprobe measurements, where usually less than a few centimeters is available between the focusing optics and/or order-selecting aperture and the sample (Ahmed *et al.*, 2000; Hayakawa *et al.*, 2000). On the other hand, the continuous monitoring of the focused microbeam is very important for checking the good alignment of the optical elements during the measurement. Another important requirement for beam-intensity monitoring is not to introduce any additional disturbing effect/element into the beam, especially in the case of microdiffraction experiments, although the detector should give a large enough signal to obtain an acceptably small (<0.1%) statistical error of the measured current.

In order to fulfill these requirements a miniature ionization chamber was constructed at the European Synchrotron Radiation Facility (ESRF) and was tested at the ID18F user end-station dedicated to precise and reproducible microprobe measurements. The size of the small monitor was optimized for microprobe measurements. The entrance window of the mini-chamber is defined by a 50 µm pinhole, which ensures the small available size and thus space between the aperture and the monitor. The technical characteristics of the small detector, such as the voltage–current characteristics, the linearity to the intensity change of the incoming beam and the stability, were tested. The results are reported in the following.

2. Technical description

A schematic drawing showing the structure of the ionization chamber can be seen in Fig. 1. The detector is composed of two guarded electrodes constructed on a polyimide printed circuit board together with the connections to the high voltage and the current read-out. The guarded electrodes, which are at a distance of 2 mm from each other, are enclosed in a small Al vessel of total thickness 10 mm along the beam and width 5 mm perpendicular to it. The 60 mm height of the vessel makes it possible to introduce the monitor into the focused beam; the monitor can be placed very close to the sample while attached to two linear motors for alignment purposes. The length of the active volume, which is determined by the length of the electrodes, is 4 mm along the direction of the focused beam. The entrance and exit windows of the chamber are defined by two Pt pinholes of diameters 50 and 300 µm, without any window material. The 50 µm diameter of the entrance pinhole allows the monitor to be positioned at ≤ 30 mm from the sample when using focusing elements with focal distances of ≥ 500 mm. Both apertures are fixed 5 mm above the lower edge and in the middle of the 5 mm side of the vessel. The microbeam passes the chamber in the axis of the apertures at 1 mm from both electrodes, thus the effect of the fluctuation of the beam position (± 0.025 mm) determined by the radius of the entrance pinhole is negligible. The ionization chamber is used with a constant Ar flow of about 1 atm pressure (the gas escapes from the chamber through the aperture of the pinholes) in order to obtain higher absorption within the detector volume.

The relative statistical error of the measured current of the ionization chamber should be less than 0.1% in order to obtain acceptable precision of the normalized measured signal. The achievable lowest statistical error of the current depends on the number of electron–ion pairs created by the X-ray beam within the active volume of the small ionization chamber. The fluctuation $\Delta N_{\rm ion}$ of the number of created electron–ion pairs $N_{\rm ion}$, and hence the current fluctuation Δi, is determined by Poisson statistics,

$$\Delta i/i = (\Delta N_{\rm ion}\, q)/(N_{\rm ion}\, q) = (N_{\rm ion})^{1/2}/N_{\rm ion}, \qquad (1)$$

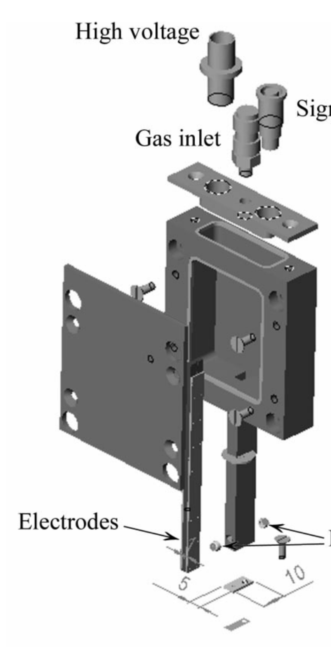

Figure 1
Technical drawing of the small ionization chamber detector. The dimensions are given in millimeters. See text for details.

where q is the electric charge of the electron.

In order to obtain $\leq 0.1\%$ relative statistical error of the measured current value, $N_{\rm ion}$ must be $\geq 10^6\ {\rm s}^{-1}$.

The number of electron–ion pairs created by N_0 X-ray photons penetrating into the active volume of the monitor in 1 s can be expressed as

$$N_{\rm ion} = N_0\{1 - \exp[-d \cdot \mu_{\rm en}(E_0)]\}E_0/W, \qquad (2)$$

where d is the active length of the ionization chamber, $\mu_{\rm en}(E_0)$ is the linear energy absorption coefficient of Ar for the incoming beam of energy E_0 and W is the average energy necessary for the creation of one electron–ion pair [W = 26.4 eV for Ar of 1 atm pressure (Knoll, 1989)]. It can be seen from (1) and (2) that the number of electron–ion pairs at a given X-ray energy is determined by the 4 mm active length of the chamber if the pressure and temperature of the Ar gas are kept constant.

The prototype of the small-beam monitor has been designed to work in the 6–28 keV energy range at the ID18F end-station, where the number of photons in the focused beam is in the 10^9–10^{10} photons ${\rm s}^{-1}$ range. This set-up results in $>10^{10}$ created electron–ion pairs per second in the 6–28 keV range (see Fig. 2) and thus the relative statistical error due to the pair-production process within the monitor is $\Delta i/i = 10^{-5}$–10^{-6}, which is always smaller than the required $<0.1\%$ relative statistical error.

3. Experimental

The test measurements were performed at the ID18F microprobe end-station of the ESRF (Somogyi *et al.*, 2001). ID18F uses the optics infrastructure of the ID18 beamline: the energy of the monochromatic X-ray beam illuminating the sample can be tuned in the 6–28 keV range by changing the undulator gap and employing a fixed-exit double-crystal Si(111) monochromator (Rüffer & Chumakov, 1996).

The experiments were performed with a monochromatic beam in the 14.4–27 keV energy range using a focused beam at 21 and 27 keV or non-focused radiation using the entrance pinhole of the chamber for defining the diameter of the measured beam. At energies of 21 and 27 keV, compound refractive lenses (CRL) (Lengeler *et al.*, 1999; Snigirev *et al.*, 1996) consisting of 64 and 94 individual Al lenses, respectively, were used for focusing.

The monitor was used with a constant Ar gas flow at 1 atm pressure controlled by a double-stage pressure reducer in order to increase the ionization density within the small volume of the chamber and to decrease the instability effects due to the variation of the pressure and humidity of the measuring gas itself. The readout electronics chain consisted of a high-precision picoammeter (Keithley 486) of sensitivity 10 fA and accuracy $<0.3\%$, an ultra-high-linearity 8-bit 1 MHz voltage-to-frequency converter (NOVA) and a VCT6 VME six-channel counter/timer (ESRF). The ionization chamber was used in direct-current mode during the measurements. In order to test the linearity of the monitor an additional photodiode was introduced into the X-ray microbeam after the small ionization chamber (see Fig. 3).

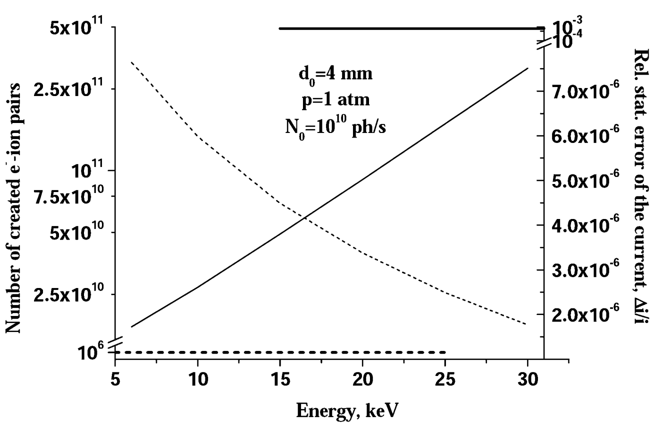

Figure 2
Dashed lines: number of created electron–ion pairs within the 4 mm active volume of the mini ionization chamber as a function of the energy of the incoming beam. Straight line: relative statistical error of the current value. See details in the text.

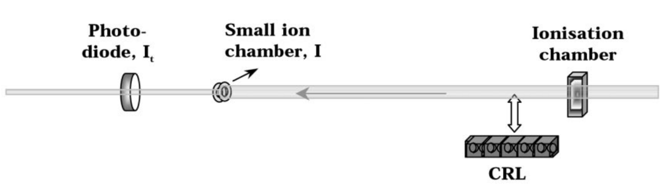

Figure 3
Experimental set-up of the test measurements of the small ionization chamber detector.

4. Experiments and results

The current–voltage characteristics curve measured at 27 keV (see Fig. 4) shows the flat plateau of the ion saturation region between 50 and 1000 V with a constant current value. Measurements of the current–voltage characteristics at different intensities and energies show that 100–150 V can be chosen as a working voltage. This is enough for suppressing the recombination to a negligible level according to the voltage–current characteristics (Knoll, 1989), since at this voltage the constant plateau has already been reached. Assuming that the electrodes are parallel plates, the electric field intensity within the two electrodes of the chamber, neglecting the space charge effect, is $E = 100\,{\rm V}/2\,{\rm mm} = 5\times10^4\ {\rm V\ m}^{-1}$, which falls into the typical range used for ionization chambers. At high enough fields there is an internal parallel-plate signal amplification as can be

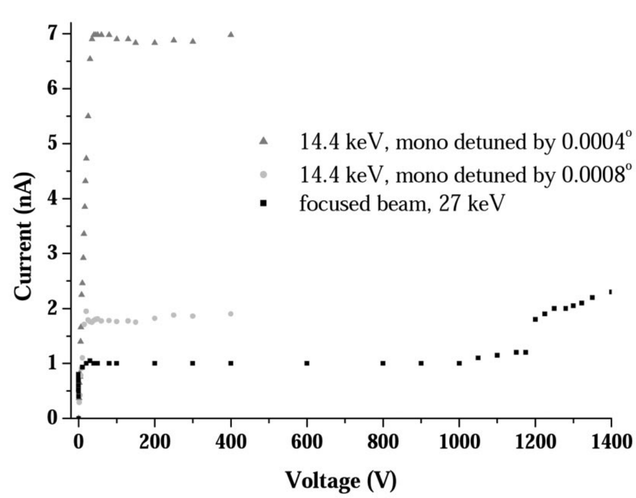

Figure 4
Current–voltage characteristics of the small ionization chamber, measured at different energies and intensities. Squares: 27 keV, beam focused by CRL of 94 lenses. Circles and triangles: 14.4 keV, unfocused beam. Note the signal amplification from ~1000 V.

seen in Fig. 4 at >1000 V voltage. The zero-offset current measured without any ionization beam was in the <20 fA range, four orders of magnitude smaller than the value of the typically measured signal.

The expected current value of the chamber can be estimated if the number of incident photons is known [see (1) and (2)]. Clearly the number of created electron–ion pairs, and thus the measured current, depends on the material, pressure and temperature of the filling gas, on the active length of the ion chamber, and on the energy and flux of the incoming photons. The effect of the change of the filling gas pressure on the number of created electron–ion pairs and thus on the measured current value can be estimated by calculating the change of the linear energy absorption coefficient as a function of the change of the pressure. The linear energy absorption coefficient can be expressed as the product of the pressure-independent mass absorption coefficient $\mu_{\rm en}(E_0)/\rho$ and the density ρ of the filling gas: $\mu_{\rm en}(E_0) = [\mu_{\rm en}(E_0)/\rho]\rho$. The change of the density and thus of the linear energy absorption coefficient of the filling gas depends linearly on the change of the pressure Δp according to the ideal gas law,

$$\mu_{{\rm en},p\pm\Delta p}(E_0) = (1 \pm \Delta p/p)\mu_{{\rm en},p}(E_0). \tag{3}$$

Since $\mu_{{\rm en},p\pm\Delta p}(E_0)d \leq 0.16$ in the energy and pressure range used at ID18F because of the small active length of the chamber, the number of absorbed photons can be approximated by [see (2)]

$$\begin{aligned} N_{{\rm abs},p\pm\Delta p} &= N_0\{1 - \exp[-\mu_{{\rm en},p\pm\Delta p}(E_0)\,d]\} \simeq N_0\mu_{{\rm en},p\pm\Delta p}(E_0)\,d \\ &= N_0\mu_{{\rm en},p}(E_0)(1 \pm \Delta p/p)\,d = N_{{\rm abs},p}(1 \pm \Delta p/p). \end{aligned} \tag{4}$$

Equation (4) shows that the fluctuation of the pressure of the filling gas linearly affects the variation of the number of absorbed photons. Therefore a very stable pressure reducer (Air Liquide) was utilized during the experiments, which made the stabilization of the pressure of the filling gas possible with <1% precision. Changing the pressure of the filling gas in the maximum achievable $\Delta p = \pm 0.039$ atm range of the pressure reducer did not significantly affect the measured current of the mini ionization chamber.

The effect of the temperature variation ΔT on the number of created electron–ion pairs can be estimated similarly,

$$\begin{aligned} N_{{\rm abs},T\pm\Delta T} &\simeq N_0\,d\,\mu_{{\rm en},T\pm\Delta T}(E_0) \\ &= [N_0\mu_{{\rm en},T}(E_0)\,d]/(1 \pm \Delta T/T) \\ &= (N_{{\rm abs},T})/(1 \pm \Delta T/T). \end{aligned} \tag{5}$$

Since the possible change of the temperature of the experimental hutch does not exceed ± 1 K the relative change in the number of absorbed photons is $\leq 0.4\%$.

The current values measured at different energies using a non-focused beam together with the values estimated on the basis of the photon flux measured by the staff of the ID18 beamline (http://www.esrf.Fr/exp_facilities/ID18/) are plotted in Fig. 5. The number of photons penetrating the active volume of the small ionization chamber is determined by the area of the entrance pinhole and the intensity distribution of the X-ray beam at 59 m from the source. In the case of measurements with a non-focused X-ray beam, the intensity distribution of the full beam at 59 m from the source at ID18 was assumed to be Gaussian with H × V = 1 mm × 2.5 mm FWHM. It can be seen from the figure that the calculated current values are in good agreement with the measured values. Thus, on the basis of the measured current values, a reliable estimation of the flux of the photon beam penetrating the active volume of the counter can be given.

In order to test the linearity of the measured current of the small ionization chamber as a function of the intensity of the incoming beam, an additional photodiode was placed into the focused beam after the small chamber (see Fig. 3). An intensity change of the focused beam of 21 keV focused by a CRL consisting of 64 individual lenses was monitored for several days. The intensity of the incoming beam at the ionization-chamber position is affected not only by the decrease of the intensity of the synchrotron current but also by the monochromator and misalignment of the focusing device. The monitored intensity varied within about two orders of magnitude, especially after the refill of the synchrotron ring during the investigated period. In Fig. 6 the current measured by the small ion chamber is plotted as a function of the current of the photodiode. Clearly the currents measured by the two detectors are linearly proportional to each other over the two order intensity range investigated.

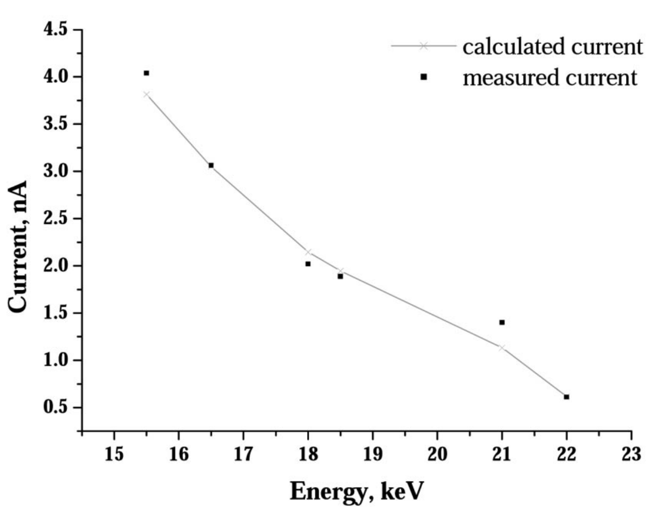

Figure 5
Measured and estimated current values of the small ionization chamber at different energies for a non-focused incoming beam.

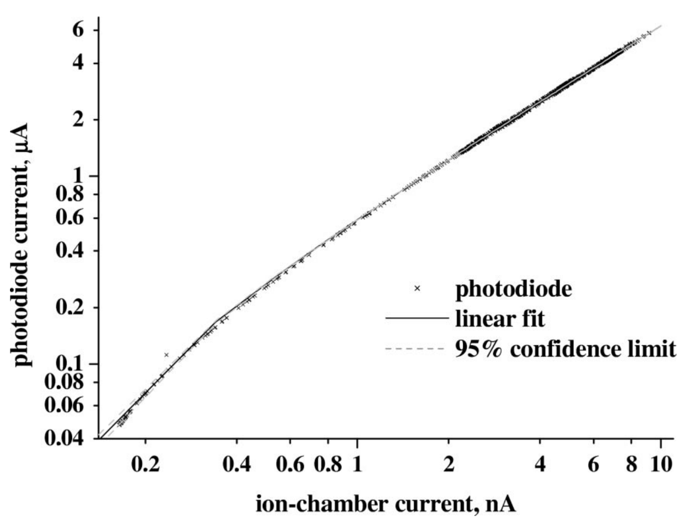

Figure 6
Measured current values of the photodiode as a function of the current of the mini ionization chamber. The beam of 21 keV was focused by a CRL of 64 individual lenses. The data are plotted in double logarithmic scale for better visualization of the covered current range.

5. Conclusion

A small windowless ionization chamber has been constructed for monitoring the intensity of the focused microbeam during microprobe measurements at the ESRF. The small dimensions of the chamber (10 mm along the beam and 5 mm perpendicular to it) make it possible to place the chamber very close (<30 mm) to the sample to be measured without cutting the focused beam. In spite of the very small active length of the device (4 mm), the created signal is well above (four orders of magnitude) the detection limit of the Keithley 486 current amplifier used for the current amplification. The current–voltage characteristics show that the small detector can be operated at a relatively low working voltage (100–150 V). The measured current values were in good agreement with the estimated values. Measuring the intensity change of the focused beam for several days proved that the current of the chamber follows linearly the intensity change in the investigated 0.1–10 nA current range.

The authors are grateful for the help of John Surr, Eric Gagliardini and Francois Fihman during the technical development of the small ionization chamber. They would like to thank the staff of the ID18 beamline for their help during the measurements at the ID18 beamline. This work was partly financed by the 'Micro-XRF' Fifth Framework EEC project under contract No. G6RD-CT-2000-00345.

References

Ahmed, S. N., Besch, H. J., Walenta, A. H., Pavel, N. & Schenk, W. (2000). *Nucl. Instrum. Methods*, A**449**, 248–253.

Hayakawa, S., Kobayashi, K. & Gohshi, Y. (2000). *Rev. Sci. Instrum.* **71**, 20–22.

Knoll, G. F. (1989). *Radiation Detection and Measurements.* NewYork/Chichester/Brisbone: John Wiley and Sons.

Lengeler, B., Schroer, C., Tummler, J., Benner, B., Richwin, M., Snigirev, A., Snigireva, I. & Drakopoulos, M. (1999). *J. Synchrotron Rad.* **6**, 1153–1167.

Rüffer, R. & Chumakov, A. I. (1996). *Hyperfine Interact.* **97**/**98**, 589–604.

Snigirev, A., Kohn, V., Snigireva, I. & Lengeler, B. (1996). *Nature* (*London*), **384**, 49–51.

Somogyi, A., Drakopoulos, M., Vincze, L., Vekemans, B., Camerani, C., Janssens, K., Snigirev, A. & Adams, F. (2001). *X-ray Spectrom.* **30**, 242–252.

 Received 1 August 2002 • Accepted 30 October 2002